Proc. 11th European Conference on Integrated Optics (ECIO '03), Prague, April 2003, vol. 1, p. 167

Frequency Shifted Feedback Ti:Er:$LiNbO_3$ Waveguide Laser of Wide Tunability

S. Reza, H. Herrmann, V. Quiring, R. Ricken, K. Schäfer, H. Suche, and W. Sohler
Angewandte Physik, Universität Paderborn, D-33098 Paderborn, Germany.
sol_sr@physik.uni-paderborn.de

An integrated, tunable frequency shifted feedback laser with Ti:Er:$LiNbO_3$ waveguide is demonstrated. The intracavity integrated acoustooptical filter used for tuning (from 1530 to 1577 nm) imposes a frequency shift on each round trip. The result is a broadened emission spectrum (FWHM=170 pm) without any longitudinal mode structure.

Keywords: acoustooptical filter, frequency shifted feedback laser, integrated waveguide laser, tunable laser, Ti:Er:$LiNbO_3$.

Introduction

In normal lasers, the oscillating optical field inside the cavity reproduces in amplitude and phase after each roundtrip at a discrete set of frequencies called longitudinal modes. This resonance condition is no longer required, if the intracavity field is frequency shifted during each roundtrip. By combining this frequency shifting with intracavity tunable bandpass filtering, a tunable frequency shifted feedback (FSF) laser can be realized. Using a bulk acoustooptical modulator this concept has already been demonstrated [1]. Such FSF lasers provide emission with low coherence length, which offer a variety of potential applications for instance in optical frequency domain ranging [2] and different types of measurement and sensing techniques [3-5]. We report on the first FSF Ti:Er:$LiNbO_3$ waveguide laser which utilizes a monolithically integrated acoustooptical wavelength filtering for frequency shifting and tuning simultaneously.

Laser design and operation principle

A schematic diagram of the laser is shown in Fig. 1. It has a Ti-indiffused channel waveguide structure in the Er diffusion-doped surface of a 94 mm long X-cut (Y-propagating) $LiNbO_3$ substrate. If optically pumped by an external laser diode (λ=1480 nm) intracavity optical amplification can be obtained in the wavelength range 1530 – 1577 nm.

The tuning element of the laser is an intracavity monolithically integrated acoustooptical filter. It consists of two polarization splitters and an acoustooptical mode converter with a tapered acoustical directional coupler in between [6]. Narrow-band wavelength filtering ($\Delta\lambda_{FWHM} \approx 2.3$ nm) is achieved by a wavelength selective (phase-matched) acoustooptical polarization conversion in combination with appropriate polarization filtering.

The polarization splitters are designed to route TM-polarized light to the bar-state and TE-polarized light to the cross-state. Thus wavelength filtering is achieved between the upper left channel and the lower right intracavity guide. The internal laser field follows the path marked by dots, if the laser structure is pumped via the lower left guide in TM-polarization. As a consequence the state of polarization (SOP) of the internal laser field is TE on the left and TM on the right. Alternatively, a TE-polarized pump selects the upper channel in the filter structure and therefore leads to a TE-polarized laser output with orthogonal SOPs internally in comparison with those indicated in the figure.

A frequency upshift is obtained for a collinear (contralinear) acoustooptical polarization conversion with a TE-polarized (TM-polarized) input field; this corresponds to the mode of operation as indicated in Fig. 1. During one round trip the laser field undergoes two polarization conversions with two frequency shifts in the same direction. The spectral width of the filter for net intracavity gain determines the effective number of round-trips and, therefore, the spectral width of the laser emission. On the other hand, a frequency downshift occurs if the device is pumped in TE-polarization and the orthogonal SOPs are observed internally. Contrary to a conventional laser, the internal laser field is not reproduced in amplitude and phase after each round-trip. The frequency shifted feedback broadens the spectral width of the laser and suppresses the formation of resonant longitudinal cavity modes.

The laser cavity is formed by two dielectric multilayer mirrors deposited on the waveguide end faces. Only the end face of the lower arm of the left polarization splitter is anti-reflection coated which facilitates efficient pump power coupling from a fiber-coupled Bragg-grating stabilized laser diode.

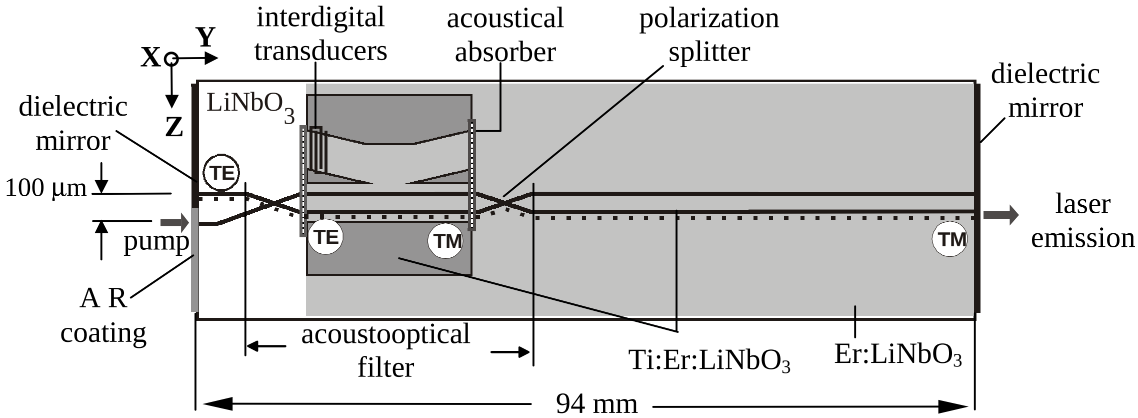

Fig. 1. Schematic diagram of the acoustooptically tunable Ti:Er:$LiNbO_3$ laser. The acoustooptical filter serves as intracavity polarization converter and frequency shifter simultaneously. The path of the intracavity laser field is indicated by dots along the waveguides optically pumped in TM-polarization.

Fabrication

At first, a planar 21.1 nm thick vacuum deposited Er-layer, covering about 80 mm of the 94 mm long sample surface, has been indiffused at 1130°C during 150 hours. In the next step, photolithographically defined 110 µm-wide acoustical waveguides have been fabricated by defining its ‘cladding’ via a deep indiffusion of 160 nm thick evaporated Ti-stripes at 1060°C during 24 hours. Then the optical waveguide structure together with the polarization splitters have been embedded symmetrically in the core of the acoustic waveguide: photolithographically defined 7 µm wide Ti stripes of 104 nm thickness have been indiffused at 1060°C during 7.5 hours. Typical waveguide scattering losses are ~0.05 dB/cm (TM-polarization) and 0.1 dB/cm (TE-polarization). Excess losses due to the polarization splitters are below 0.5 dB. Afterwards broadband (1.2 µm < λ < 2.0 µm) antireflection coatings have been deposited on both ends of the sample to avoid reflections during characterisation of the polarisation splitting ratios and to facilitate the pump coupling.

Interdigital transducers with 20 finger pairs have been fabricated by aluminium sputtering using the lift-off photolithography technique. An impedance matching circuit allows to excite the SAW with high efficiency. Then the acoustooptical filter characteristics has been studied to determine the phase matching frequencies and RF-power levels for best conversion efficiency. Finally, high reflection broadband dielectric mirrors of about 97.5% reflectivity (1450 nm < λ < 1700 nm) have been deposited on the end faces of both waveguides on the right and on the end face of the upper waveguide on the left (see Fig. 1.).

Laser operation

The laser is pumped using a fiber-coupled Bragg-grating stabilized laser diode of 1480 nm wavelength providing an output power up to 135 mW. The polarization of the pump radiation is adjusted either to TM or TE polarization using a fiber optical polarization controller. Fig. 2a shows the measured power characteristics at ~ 1564 nm emission wavelength as laser output power versus incident pump power. The results of both modes of operation are presented in Fig 2a for TM- (TE-) polarized pump leading to TM- (TE-) polarized output. The threshold pump power of the laser is ~ 50 mW (TM) and at ~ 70 mW (TE). The low slope efficiency of about 1.5×10^{-3}, leading to a maximum output power 120 µW (TM) and 75 µW (TE), respectively, demonstrates a large potential for further optimisation.

The emission wavelength of 1564 nm is determined by the surface acoustic wave (SAW) frequency of ~ 170 MHz; the corresponding electrical drive power for complete polarization conversion is about 80 mW. Tuning of the emission wavelength is achieved by adjusting the SAW-frequency. Continuous tuning could be demonstrated in the wavelength range 1530 nm < λ < 1577 nm with a tuning slope of about –8 nm/MHz. Due to the wavelength dependence of gain, losses, acoustooptical conversion efficiency and mode overlap the laser output power strongly varies as function of the emission wavelength (or SAW-frequency) (see Fig. 2b).

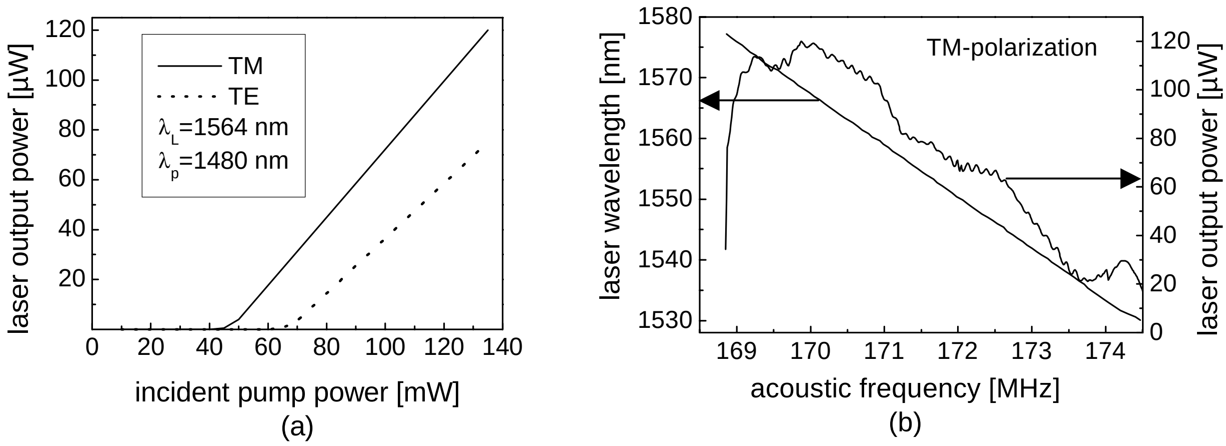

Fig. 2: (a) Laser output power versus incident pump for two modes of operation in TM- and TE-polarization, respectively. (b) laser emission wavelength (left ordinate) and output power (right ordinate) versus SAW-frequency at 135 mW of pump power in TM-mode of operation.

A frequency shifted feedback laser emission has completely different spectral characteristics compared to a normal laser. In Fig. 3a (Fig. 3b) the measured emission spectrum of the FSF laser is shown for TM (TE) pump polarisation. The chosen resolution of the spectrum analyzer of 10 pm would allow to identify a longitudinal mode spectrum of the 94 mm long cavity. The measurements however, clearly show modeless spectra of about 0.17 nm width (FWHM) with very smooth envelopes confirming FSF laser operation. The envelopes are slightly asymmetric. As a result of the frequency upshift for TM-polarization, the envelope of the spectrum is steepened at the short wavelength side (higher frequencies) (Fig. 3a), whereas downshifting in the TE-case results in a steepening on the longer wavelength side (Fig. 3b).

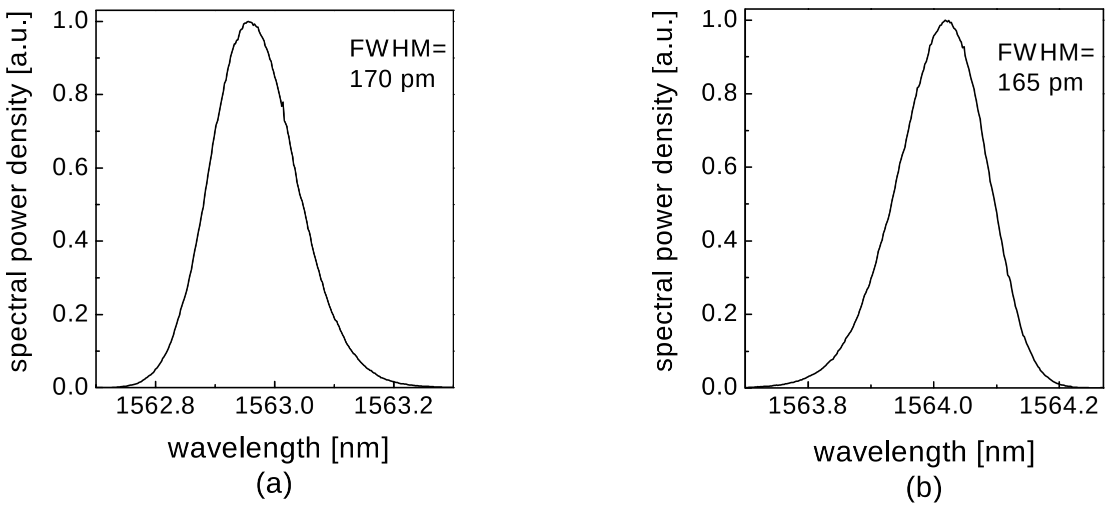

Fig. 3. Spectra of the frequency shifted feedback laser taken with a 10 pm resolution, (a) pump and emission TM-polarized and frequency upshifted (b) pump and emission TE-polarized and frequency downshifted.

Conclusions

We have demonstrated for the first time tunable frequency shifted feedback operation of a Ti:Er:$LiNbO_3$ waveguide laser. Intracavity frequency shifting and tuning over 47 nm have been achieved using the monolithically integrated acoustooptical filter. The smooth envelope of the output spectra (FWHM=0.17 nm) clearly show a modeless laser operation as expected for FSF lasers. Further detailed investigations including theoretical modeling are required to optimize laser performance.

Acknowledgement

This work has been supported by the Deutsche Forschungsgemeinschaft as one project of the research group ‘Integrated Optics in Lithium Niobate: New Devices, Integrated Circuits and Applications’.

References

[1] I. C. M. Littler et al., *J. Opt. Soc. Amer. B*, **8**, 1412-1420, 1991

[2] K. Nakamura et al., *IEEE J.Quantum Electron.* **36**, 305-316, 2000.

[3] J.R.M. Barr et al., *Optics Lettrs*, **18**, 1010-1012, 1993.

[4] M Yoshida et al., *IEEE Photon. Technol. Lett.*, **13**, 227-229, 2001

[5] K. Iiyama et al., *IEEE J. Select. Top. Quantum Electron.* **7**, 484-489, 2001.

[6] H. Herrmann et al., *J. Lightwave Technol.*, **13**, 364-374, 1995.